Available online at www.sciencedirect.com

ScienceDirect

IFAC PapersOnLine 55-7 (2022) 969–974

Control of steam bottoming cycles using nonlinear input and output transformations for feedforward disturbance rejection ⋆

Cristina Zotică * **Rubén M. Montañés** * **Adriana Reyes-Lúa** * **Sigurd Skogestad** **

* *SINTEF Energy Research, Sem Sælandsvei 11, 7034, Trondheim, Norway*

** *Department of Chemical Engineering, Norwegian University of Science and Technology (NTNU), Sem Sælandsvei 4, 7491, Trondheim, Norway*

Abstract: In this paper we analyze the control problem for a steam cycle that produces power by recovering waste-heat from gas turbines on an offshore installation. The waste-heat recovery unit is based on once-through steam generator technology. The main disturbances are large variations of the gas turbine exhaust gas flowrate and temperature. We analyze the effect of these disturbances on the operation of the steam cycle, specifically for the superheated steam pressure and temperature. We compare the performance of different decentralized control strategies based on standard PID-controllers and nonlinear feedforward. We consider floating pressure and constant pressure operation strategies. For steam temperature control we implement feedback, and feedback in combination with nonlinear input and output transformations for feedforward disturbance rejection. These transformations are based on the steady-state energy balance on the waste heat recovery unit, while for simulation purposes we use a high-fidelity dynamic model of the bottoming cycle designed to minimize the weight and volume. The outcome from this work can be used to propose control strategies for coordinating a combined cycle (gas turbine with a steam bottoming cycle) that can operate with large and rapid changes in power demand.

Keywords: nonlinear control, feedforward disturbance rejection, steam cycles

1. INTRODUCTION

Gas turbines are the main source for generating electrical and mechanical power, as well as heat, in offshore oil and gas extraction installations. On the Norwegian Continental Shelf (NCS), gas turbines are the highest greenhouse gas emission source, with a share of 84.95 % in 2020 (Norwegian Petroleum Directorate, 2021). Figure 1 shows a simplified process flowsheet of a more efficient combined cycle for producing power. In Figure 1, fuel is combusted with air to produce high temperature and pressure gas which is expanded in a gas turbine (GT) which drives a power generator. The temperature of the exhaust gas from the gas turbine is sufficiently high (400 °C to 500 °C) to have a high potential for waste-heat recovery. This can be done, for example, by generating high-pressure superheated steam in a boiler, which can then be expanded in a steam turbine (ST) to drive a generator to produce additional power. The low-pressure steam is condensed using seawater as cooling utility. By installing a combined cycle, more power can be produced with the same given amount of fuel, and therefore the energy efficiency is increased and the CO_2 intensity [$kgCO_2\,J^{-1}$] is reduced. Note that steam may be extracted from the turbine for heating purposes at intermediate pressure levels, but in this work we focus on a steam bottoming cycle producing power only.

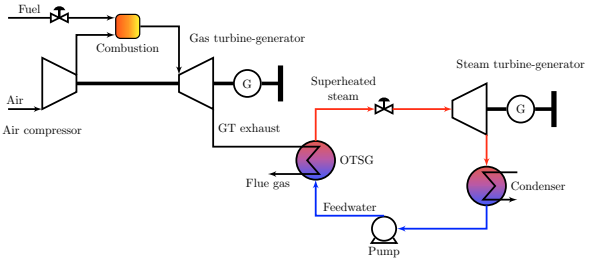

Fig. 1. Simplified process flowsheet of a combined cycle with a gas turbine and a steam bottoming cycle. In this work we focus on the steam bottoming cycle which includes the boiler (once-though steam generator (OTSG)), steam turbine, condenser and pump.

Compactness is a key decision factor for deploying equipment in oil and gas extraction installations, and the additional weight of a steam cycle compared to a gas turbine can be considered a drawback. Therefore, bottoming steam cycles for offshore applications need to be designed for minimum weight and volume. A way to reduce the size of the system is to design the boiler in Figure 1 as a

⋆ This publication has been produced with support from the LowEmission Research Centre (www.lowemission.no), performed under the Norwegian research program PETROSENTER. The authors acknowledge the industry partners in LowEmission for their contributions and the Research Council of Norway (296207).

10.1016/j.ifacol.2022.07.570

once-through steam generator (OTSG), with a single heat exchanger for all three phase regimes, i.e., from subcooled water to saturated steam and further to superheated steam (Nord et al., 2014; Deng et al., 2021). In addition, the selection of smaller tube diameter in tube bundles compared to standard onshore tube sizes together with further design optimization might lead to significant reductions in OTSG weight and volume (Montañés et al., 2021). However, by reducing the size of the steam generator, and therefore its hold-up and thermal inertia, additional control and operational challenges arise. For example, disturbances in the gas turbine exhaust flowrate and temperature caused by fast load changes lead to large variations of the superheated steam temperature and pressure and therefore operational issues for the steam turbine (Montañés et al., 2021). Reliable power generation is critical for offshore operation, and therefore, the combined cycle must be able to provide fast load changes to keep the power system stable under unforeseen events, including load rejection of unplanned trips of large direct drive electrical motors. For this reason, in offshore oil and gas applications, bottoming cycles need to be set up for flexible operation to cover varying power demands across multiple time scales.

The operational objective of the bottoming cycle is to produce power by processing a given amount of waste-heat in the exhaust of the gas turbine. In this context, the objective of this work is to study different control strategies for controlling superheated steam pressure and temperature in a steam bottoming cycle subjected to large heat input variations (disturbances). We compare constant pressure and floating pressure operation modes, which are standard in onshore heat-to-power cycles (Zotică et al., 2020b). In the latter, the pressure is uncontrolled and varies with the heat input. For temperature control, we consider feedback control and a type of model-based nonlinear feedforward control, which uses input and output transformations (Zotică et al., 2020a; Zotică and Skogestad, 2021).

Model based feedforward is commonly found in control structures of steam cycles (i.e., power plants). Once such example is the *3-element control* scheme for drum-boilers. Here, the level is controlled by manipulating the feedwater flowrate. In addition to the level feedback signal, there is a feedforward signal with the difference between the steam and feedwater flowrates (Lindsley, 2000). Shinskey and Louis (1968) patented a control strategy from a once-through steam boiler which employs mass and energy balance calculation blocks. Welfonder (1999) presents the use of dynamic model-based calculation blocks to coordinate the setpoints for pressure and power for given power-plant load. For compact bottoming cycles, the work by Nord and Montañés (2018) suggests the use of feedforward control combined with feedback as an effective means of controlling superheated steam temperature, while the work by Montañés et al. (2021) indicates that implementing feedforward effectively might be challenging for operators. (Camacho, 2012) summarizes different methods for controlling the steam temperature generated in a solar collector by manipulating the water flowrate. These include nonlinear feedforward derived from steady-state energy balance.

However, despite the extended use of model-based calculation blocks in industry, a systematic theory to derive such blocks is missing from the open literature. This is the goal of recent work in (Zotică et al., 2020a; Zotică and Skogestad, 2021), and continued in Skogestad et al. (2022a) and in Skogestad et al. (2022b), and it is the framework we apply in this paper.

2. DYNAMIC MODEL FOR COMPACT STEAM BOTTOMING CYCLES

The real system is more complex than shown in Figure 1. Heat is recovered from two SIEMENS SGT750 gas turbines, operated in synchronous mode, and 90 % load of the gas turbines is selected as the design point of the bottoming cycle. Two OTSGs, designed to minimize weight given a desired power production, are operated in parallel and feed steam to a common steam turbine and condenser system. For the simulations we use a detailed DAE model developed in the Modelica language and implemented in Dymola (Dassault Systèmes, 2019; Dempsey, 2006) together with the numerical solver Dassl. We model in detail the two OTSGs, while the exhaust of the gas turbines is a boundary condition. We assume ideal gas for the exhaust gas, and to model its thermodynamic properties, we use the NASA Gleen representation, with a 6^{th} order polynomial for individual species (McBride et al., 2002). We model the water (and steam) thermodynamic properties using the IF97 standard as reference (Åberg et al., 2017).

The detailed dynamic model of the compact OTSG and the design optimization method are described in detail in previous work by Montañés et al. (2021). The model is based on a 1D approach for dynamic modelling and simulation of heat recovery steam generators as suggested by Dechamps (1995). The condenser is a shell and tube heat exchanger, assuming thermodynamic equilibrium between liquid and vapor phases, with cooling water and steam/condensate separated by a dynamic wall model.

Each steam turbine section is modeled by two main sub-models as suggested by Celis et al. (2017), namely, a lumped steam storage volume at the inlet and a turbine section with thermal and quasi-static flow characteristics. This is a reasonable approximation, as the response time of the steam turbine is relatively short compared to the response time of the OTSG. Thermal expansion in a given steam turbine section is modeled by means of the isentropic efficiency relation. For the condensing stages, the Baumann correction is used to account for the effect of moisture on efficiency (Bolland, 2014). The flow characteristics of the turbine section are calculated by means of the empirical correlation defined by Stodola's cone law (Cooke, 1985), which defines the swallowing capacity of the turbine when operating the turbine under off-design conditions. Variable speed pumps with quadratic flow characteristics are implemented. Valves consider compressible fluid with possible choked flow conditions.

3. NONLINEAR INPUT AND OUTPUT TRANSFORMATIONS

We present here a summary for the theory for transformed inputs and outputs. Figure 2 shows the proposed method for input transformation. In Figure 2, y is the output vector, u is the original input vector, v is the transformed input

vector, and d is the disturbance vector. We may also include some measured states w. The transformed input v is given by a static function of the other variables

$$v = g(u, y, w, d) \tag{1}$$

The function g is yet to be defined, but in the ideal case it transforms a nonlinear system into a linear system from v to y that is decoupled and that also has feedforward disturbance rejection (Zotică et al., 2020a; Skogestad et al., 2022a). This theory is closely related to the nonlinear control theory of feedback linearization (Isidori, 1989), but it focuses on feedforward disturbance rejection.

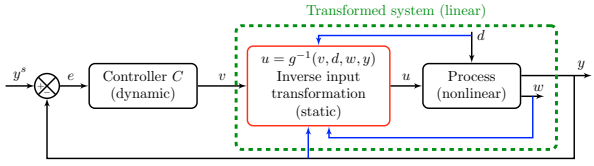

Fig. 2. Nonlinear input transformation for linearization, decoupling and feedforward disturbance rejection which in the ideal case transforms a nonlinear process into a linear and decoupled system which also has perfect disturbance rejection. y is the output vector, u is the original input vector, v is the transformed input vector, d is the disturbance vector, and w are some additional measured states.

In Figure 2, a PI-controller sets the transformed input v that keeps the output y at its setpoint y^s. Note that the signal v can also be set directly by an operator. The principle of this method is to simplify the task of either designing a control system for a nonlinear process, or the task of the operator in controlling such process. The physical input u is calculated by numerically or algebraically solving Eq.1 with given v, y, w and d. The outer controller C rejects unmeasured disturbances and accounts for plant-model mismatch.

3.1 Definition of transformed inputs and outputs

We assume that we have a $n \times n$ system with n outputs and n inputs. In addition, we assume that all disturbances d and some additional states w can be measured. A systematic way to derive these transformations is to start from the model equations, either for static (Eq. 2a), or dynamic case (Eq. 2b).

$$y = f_0(u, w, d) \tag{2a}$$

$$\frac{dy}{dt} = f(u, w, d, y) \tag{2b}$$

The transformed input can be defined for a static model as the right hand side of Eq. 2a (Eq. 3a), while for dynamic model (Eq. 3b) we introduce an additional tuning parameter $\mathcal{T}_A$ with the goal of obtaining a first-order model (see Zotică and Skogestad (2021) for choosing $\mathcal{T}_A$).

$$v_0 = \underbrace{f_0(u, w, d)}_{g(u,w,d)} \tag{3a}$$

$$v = \underbrace{\mathcal{T}_A f(u, w, d, y) + y}_{g(u,y,w,d)} \tag{3b}$$

We assume that $g(\cdot)$ is invertible.

Substituting the transformed input v_0 or v (Eq. 3) in the model (Eq. 2) and rearranging for the dynamic model, gives a transformed system that is linear, decoupled and has perfect disturbance rejection, for the static and dynamic case respectively.

$$y = v_0 \tag{4a}$$

$$\mathcal{T}_A \frac{dy}{dt} = -y + v \tag{4b}$$

In some cases, including the steam cycle analyzed in this work, we may simplify the implementation of transformed inputs v by introducing a transformed output z

$$z = h(y, u, w, d) \tag{5}$$

where h is a static function that we choose.

By introducing the transformed outputs z, the transformed inputs v can be defined as a static function of z

$$v_z = g_z(u, w, z, d) \tag{6}$$

The new transformed system in terms of the transformed input v_z and transformed output z is

$$z = v_{z0} \tag{7a}$$

$$\mathcal{T}_A \frac{dz}{dt} = -z + v_z \tag{7b}$$

for the static and dynamic case respectively.

Figure 2 applies to the transformed system in Eq. 7, except that the outer SISO-controller C controls the transformed output z.

4. TRANSFORMED INPUTS AND OUTPUTS FOR A TEMPERATURE CONTROL OF STEAM BOTTOMING CYCLE

The dynamic model described in Section 2 can be used to asses the transient performance of the system, but it is too complex to be used for model-based control purposes. Therefore, we derive the transformed variables using a steady-state energy balance and use Eq. 3a to define a static transformed input v_0. We assume that we can measure (or estimate) the disturbances and some additional states, as discussed later.

4.1 Derivation of transformed inputs and outputs for temperature control

In this work, we control $y_1 = T_s$ using the feedwater flowrate ($u_1 = m_w$), and for constant pressure operation mode, we control $y_2 = p_s$ using the turbine valve ($u_2 = z_T$). We implement nonlinear feedforward and feedback for y_1, and feedback only for y_2. For feedforward control, the disturbances are the gas turbine exhaust flowrate ($d_1 = m_g$) and the temperature of the gas inlet to the OTSG ($d_2 = T_g^i$). In addition, we assume that we can measure or estimate some states w, the feedwater specific enthalpy ($w_1 = H_w$), and the exhaust gas temperature at the outlet of the OTSG ($w_2 = T_g^o$). Note that we assume perfect measurement of the exhaust gas mass flowrate (m_g), which may not be available in practice, but it can be estimated from gas turbine measured data and characteristic curves or performance models. These models are typically available for operators.

Assuming constant specific heat for the gas (c_{p_g}) and fast mass dynamics, the steady-state energy balance for the OTSG is:

$$m_g c_{p_g}(T_g^i - T_g^o) = m_w\,(H_s - H_w) \tag{8}$$

where H_s and H_w are the specific enthalpy for steam and water, respectively. In Eq. 8, we use the specific enthalpy H_w and H_s because the process consists of a two-phase flow with phase change on the water/steam side of the OTSG and the water thermodynamics are non-ideal. On the other hand, the exhaust gas thermodynamics are assumed to be ideal (see Section 2).

Therefore, in this case, we have introduced as transformed output z the steam specific enthalpy, and as w variable the feedwater specific enthalpy:

$$z = H_s = g_z(T_s, p_s) \tag{9a}$$
$$w = H_w = g_z(T_w, p_w) \tag{9b}$$

where g_z can for example be a look-up table that computes H_w and H_s based on the measured pressure and temperature. This is a reasonable assumption because steam tables are easily available and are widely used in the industry. The setpoint for H_s^s is computed similarly. Note that we use the pressure setpoint for constant pressure operation and the measured pressure for floating pressure.

Solving Eq. 8 for H_s yields:

$$z = H_s = \underbrace{H_w + c_{p_g}(T_g^i - T_g^o)\frac{m_g}{m_w}}_{f_{0z}(u,d,w)} \tag{10}$$

The transformed input v_0 is defined as the right-hand-side of Eq. 10.

$$v_0 = f_{0z} = H_w + c_{p_g}(T_g^i - T_g^o)\frac{m_g}{m_w} \tag{11}$$

Substituting v_0 in Eq. 10, gives the transformed system

$$z = v_0 \tag{12}$$

which is linear and has no effect from disturbances. However, the real process is dynamic, so the effect of the transformation rejects disturbances perfectly only at steady-state, but not dynamically.

4.2 Implementation of transformed inputs and outputs

Solving Eq. 11 for the input $u_1 = m_w$, given disturbances d and controller output v gives:

$$m_w = \underbrace{\frac{m_g c_{p_g}(T_g^i - T_g^o)}{v_0 - H_w}}_{f_{0z}^{-1}(v,w,d)} \tag{13}$$

Eq. 13 has a singularity at $v = H_w$, but this is not very likely to happen physically, at least not in the simulations for the steam cycle or during normal operation. For a general case, the controller output v_0 could have a lower bound to prevent the singularity. Figure 3 shows the implementation for transformed inputs and outputs, where the input $u = m_w$ is computed in an algebraic block from Eq. 13.

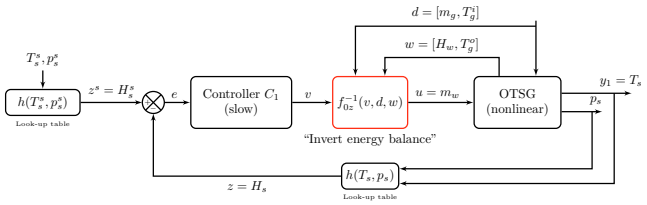

Fig. 3. Implementation of transformed inputs and outputs for steam temperature control.

5. NUMERICAL EXAMPLE OF A STEAM BOTTOMING CYCLE

In this section, we implement the control structures with transformed variables proposed in Section 4 to the dynamic model described in Section 2.

5.1 Process data

Table 1 summarizes the nominal operating conditions for the steam cycle.

Table 1. Nominal operating conditions for the steam bottoming cycle

Variable	Symbol	Value	Unit
Steam turbine power output	W	20	MW
Superheated steam pressure	p_s	23	bar
Superheated steam temperature	T_s	353	°C
Exhaust gas inlet temperature	T_g^i	443	°C
Exhaust gas outlet temperature	T_g^o	169	°C
Cooling water temperature	T_{cw}	12	°C
Feedwater inlet temperature	T_w^i	27	°C
Feedwater mass flowrate	m_w	21.9	$\mathrm{kg\,s^{-1}}$
Exhaust gas mass flowrate	m_g	225.5	$\mathrm{kg\,s^{-1}}$
Turbine valve opening	z_T	0.9	-

5.2 Controller tuning

Table 2 shows the controller tuning parameters for temperature control used for both floating pressure and constant pressure operation modes. K_c is the proportional gain and τ_I is the integral time. All controllers are tuned using the SIMC tuning rules (Skogestad, 2003) and based on step responses obtained with the simulation model described in Section 2. Note that for all structures we use in addition an inner loop flow controller that manipulates the feedwater pump rotation to keep the flow at its setpoint. This is a pure I-controller with a integral gain $K_I = 11.11$, tuned with a closed loop time constant $\tau_c = 5s$. Because of this inner flow controller and the time scale separation that we need between the two controllers, the outer controller for both strategies cannot be made faster to improve the performance.

Table 2. Controller tuning for the two temperature control structures

Control structure	K_C	τ_I [s]	τ_C [s]
Feedback only	-0.072	277	60
Feedback and feedforward	5.7	280	60

For constant pressure operation mode, we use a pure I-controller tuned on the initial gain. Using the SIMC tuning rules (Skogestad, 2003) and selecting a closed loop time constant τ_c=5 s, gives an integral gain $K_I = -0.08$.

5.3 Simulation results

We implemented the control structures proposed in Section 4.2 with the controller tunings described in Section 5.2 to the bottoming cycle dynamic simulation model described in Section 2. We analyze the performance of the proposed control structures to disturbance rejection in the gas turbine exhaust gas flowrate (Figure 4(a)) and temperature (Figure 4(b)). Both disturbances occur simultaneously, and this type of behavior corresponds to a ramp load decrease in the gas turbine.

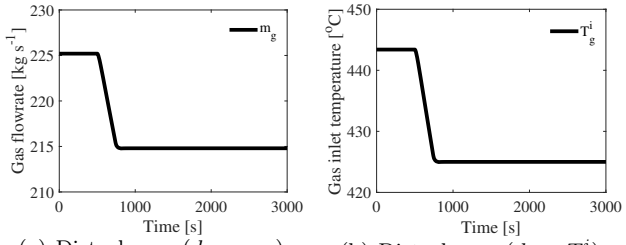

(a) Disturbance ($d_1 = m_g$) (b) Disturbance ($d_2 = T_g^i$)

Fig. 4. Disturbances in the exhaust gas mass flowrate and temperature which emulate a ramp load change in the gas turbine.

Figure 5 shows the response of the superheated steam pressure for the two proposed temperature control structures considered in this work. In Figure 5(a), the pressure is allowed to vary, and after the disturbances, it reaches a lower value at steady-state. In Figure 5(b) the pressure is kept at a constant setpoint.

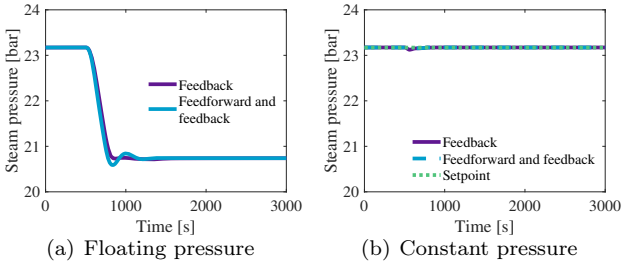

(a) Floating pressure (b) Constant pressure

Fig. 5. Comparison of steam pressure ($y_2 = p_s$) response for the two proposed temperature control structures for floating and constant pressure respectively.

Figure 6 compares the superheated steam temperature (T_s) response for the two proposed temperature control structures. Figure 6(a) shows the response for floating pressure and Figure 6(b) shows the response when the pressure is kept constant. The offset in Figure 6(a) is caused by the different pressure values used to compute the setpoint H_s^s. For floating pressure operation (Figure 6(a)), we use the pressure measurement p_s, whereas for constant pressure operation in Figure 6(b) we use the pressure setpoint p_s^s.

Figure 7 compares the response for the feedwater flowrate ($u_1 = m_w$) for the two proposed temperature control structures for floating and constant pressure operation.

Figure 8 compares the response of the power for the two proposed temperature control structures for floating and constant pressure operation.

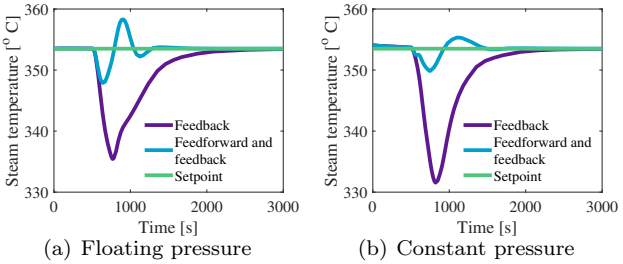

(a) Floating pressure (b) Constant pressure

Fig. 6. Comparison of steam temperature ($y_1 = T_s$) response for the two proposed temperature control structures for floating and constant pressure respectively.

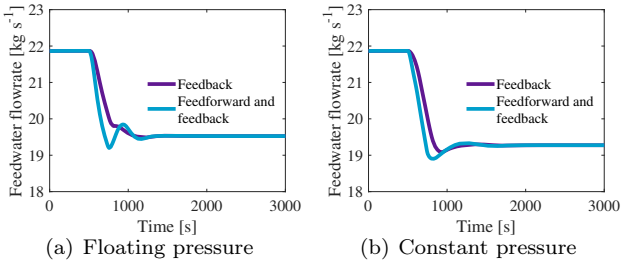

(a) Floating pressure (b) Constant pressure

Fig. 7. Comparison of feedwater flowrate ($u_1 = m_w$) response for the two proposed temperature control structures for floating and constant pressure respectively.

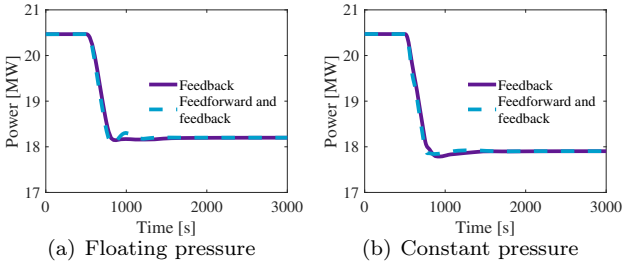

(a) Floating pressure (b) Constant pressure

Fig. 8. Comparison of steam turbine power (W) response for the two proposed control structures for floating and constant pressure respectively.

Figure 9 shows the response of the turbine valve $u_2 = z_T$ for the two proposed control structures for constant pressure operation. For floating pressure, $u_2 = z_T$ is kept at 90 % opening.

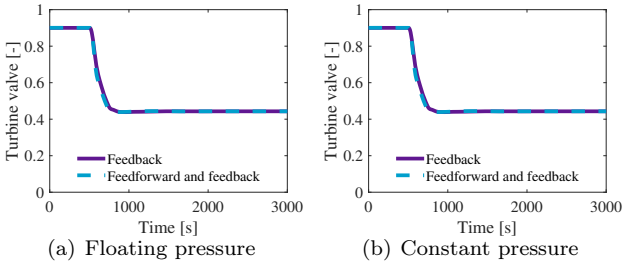

(a) Floating pressure (b) Constant pressure

Fig. 9. Turbine valve ($u_2 = z_T$) response for the two proposed temperature control structures for floating constant pressure respectively.

6. CONCLUSION

In this work, we study the control problem for a steam bottoming cycle exposed to large disturbances from the upstream gas turbine (see Figure 4). For simulations, we use a high-fidelity dynamic model developed in Dymola. We consider two pressure operation modes, floating and constant. In the former, the pressure is varying with the heat input (Figure 5(a)), while in the latter is kept at setpoint (Figure 5(b)) by manipulating the turbine valve (Figure 9(b)). The temperature responses for the feedback and feedforward control strategy in Figure 6 show an overshoot for disturbance rejection. This effect propagates to the power response in Figure 8. The root cause of this behaviour is the feedforward and outer feedback controller doing independent corrections simultaneously. This effect can be reduced by slowing down the outer feedback loop. Nonetheless, the overshoot for power is small, and, compared to feedback only, the feedforward implementation shows the smallest deviation from the steam temperature setpoint for both floating pressure and constant pressure operation modes. This is desired in order to reduce the thermal stress on the steam turbine blades and rotor. The steady-state value for power for the floating pressure operation mode in Figure 8(a) is higher than the steady-state value for the constant pressure operation mode in Figure 8(b) because of the throttling losses in the steam turbine valve.

For future work, we will analyze coordinating the combined cycle (gas turbine with a steam bottoming cycle) using decentralized control for operating with large and rapid changes in power demand.

REFERENCES

Åberg, M., Windahl, J., Runvik, H., and Magnuson, F. (2017). Optimization-friendly thermodynamic properties of water and steam. In *Proceedings of the 12th International Modelica Conference, Prague, Czech Republic*.

Bolland, O. (2014). Thermal Power Generation - Compendium. Norwegian University of Science and Technology (NTNU), Department of Energy and Process Engineering.

Camacho, E.F. (2012). *Control of Solar Energy Systems*. Advances in Industrial Control. London, 1st ed. 2012. edition.

Celis, C., Pinto, G., Teixeira, T., and Xavier, E. (2017). A steam turbine dynamic model for full scope power plant simulators. *Applied Thermal Engineering*.

Cooke, D. (1985). On prediction of off-design multistage turbine pressures by Stodola's ellipse. *J. Eng. Gas Turb. Power*.

Dassault Systèmes (2019). DYMOLA Systems Engineering. Multi-Engineering Modeling and Simulation based on Modelica and FMI.

Dechamps (1995). Modelling the Transient Behaviour of Heat Recovery Steam Generators. *Proceedings of the Institution of Mechanical Engineers, Part A: Journal of Power and Energy*, (4).

Dempsey, M. (2006). Dymola for Multi-Engineering Modelling and Simulation. In *2006 IEEE Vehicle Power and Propulsion Conference*. IEEE.

Deng, H., Skaugen, G., Næss, E., Zhang, M., and Øiseth, O.A. (2021). A novel methodology for design optimization of heat recovery steam generators with flow-induced vibration analysis. *Energy*.

Isidori, A. (1989). *Nonlinear Control Systems*. Springer-Verlag Berlin Heidelberg GmbH, second edition.

Lindsley, D. (2000). *Power-plant control and instrumentation : the control of boilers and HRSG systems*. IEE control engineering series. Institution of Electrical Engineers, London.

McBride, B.J., Zehe, M.J., and Gordon, S. (2002). Nasa glenn coefficients for calculating thermodynamic properties of individual species. *NASA/TP*.

Montañés, R.M., Skaugen, G., Hagen, B., and Rohde, D. (2021). Compact steam bottoming cycles: Minimum weight design optimization and transient response of once-through steam generators. *Frontiers in Energy Research*.

Nord, L.O., Martelli, E., and Bolland, O. (2014). Weight and power optimization of steam bottoming cycle for offshore oil and gas installations. *Energy*.

Nord, L.O. and Montañés, R.M. (2018). Compact steam bottoming cycles: Model validation with plant data and evaluation of control strategies for fast load changes. *Applied Thermal Engineering*.

Norwegian Petroleum Directorate (2021). Emissions to air.

Shinskey, F.G. and Louis, J.R. (1968). *Once-trough boiler control system*. US Patent 3,147,737. United States Patent Office.

Skogestad, S. (2003). Simple analytic rules for model reduction and PID controller tuning. *Journal of Process Control*, (4).

Skogestad, S., Zotică, C., and Alsop, N. (2022a). Nonlinear input transformations for linearization, decoupling and feedforward control - part 1. In preparation.

Skogestad, S., Zotică, C., and Alsop, N. (2022b). Nonlinear input transformations for linearization, decoupling and feedforward control - part 2. In preparation.

Welfonder, E. (1999). Dynamic interactions between power plants and power systems. *Control Engineering Practice*, (1).

Zotică, C., Alsop, N., and Skogestad, S. (2020a). Transformed Manipulated Variables for Linearization, Decoupling and Perfect Disturbance Rejection. *IFAC-PapersOnLine*.

Zotică, C., Nord, L.O., Kovács, J., and Skogestad, S. (2020b). Optimal operation and control of heat to power cycles: A new perspective from a systematic plantwide control approach. *Computers and Chemical Engineering*.

Zotică, C. and Skogestad, S. (2021). Input transformation for linearization, decoupling and disturbance rejection with application to steam networks. Computer Aided Chemical Engineering. Elsevier.